A Time–Frequency Domain Approach to Synchronization, Channel Estimation, and Detection for DS-CDMA Impulse-Radio Systems

Andrea M. Tonello, *Member, IEEE*, and Roberto Rinaldo, *Member, IEEE*

***Abstract*—This paper deals with synchronization, channel estimation, and detection in ultrawideband (UWB) biphase impulse–modulated systems. We address both the single-user scenario, and the multiuser scenario assuming a direct-sequence code-division multiple-access (DS-CDMA) scheme. The users' binary-codeword elements modulate short-duration pulses. Codewords span a transmission frame. Frames are separated by a guard time to cope with the channel time dispersion. The detection approach is single-user-based and it operates in the frequency domain (FD). The algorithm first acquires frame synchronization with the desired user. It runs a discrete Fourier transform (DFT), and it performs FD channel estimation for the desired user via a recursive least-squares (RLS) algorithm. Finally, detection is directly accomplished in the FD. Frame synchronization is achieved in the time domain with a two-step procedure that first acquires coarse timing, then finely estimates where the desired user's signal energy is located. In the presence of multiple-access interference (MAI), the algorithm is appropriately modified to include the capability of canceling the interference through the exploitation of its FD correlation. Simulation results show that the proposed approach exhibits fast convergence, and high performance with and without synchronous/asynchronous MAI.**

***Index Terms*—Channel estimation, code-division multiple access (CDMA), frequency-domain (FD) processing, impulse modulation, interference cancellation, multiuser detection, timing acquisition, ultrawideband (UWB) systems.**

I. Introduction

THIS PAPER deals with synchronization, channel estimation, and detection in impulse-radio systems [1]. Several combinations of modulation, and user-multiplexing schemes have been proposed for impulse-radio communications [2]. The common attractive feature is the carrierless baseband implementation that involves transmission of short-duration pulses. This technology is commonly referred to as ultrawideband (UWB), because the pulses can occupy a very-large bandwidth [3]. Most of the work has focused so far on schemes that deploy time-hopping spreading codes with pulse-position modulation [1]. Instead, in this paper, we assume the deployment of biphase pulse amplitude modulation (BPAM) in conjunction with direct-sequence code-division multiple access (DS-CDMA) [2], [4], [5]. Binary codewords are assigned to users, and modulate short-duration pulses (monocycles). A user's codeword spans a transmission frame. Frames are separated by a guard time to cope with the time dispersion that is introduced by the channel-frequency selectivity [1], [6].

When the guard time is longer than the channel time dispersion, and only a single user accesses the medium, the optimal receiver comprises a matched filter followed by a symbol-by-symbol threshold detector [6]. The receiver filter has to be matched to the equivalent impulse response that comprises the user's waveform, and the channel impulse response. Since UWB signals can occupy a large bandwidth, the channel is highly frequency selective, and the received signal exhibits a large number of multipath components. Potentially, high-frequency diversity gains can be achieved [6]. However, the optimal matched-filter receiver has to accurately estimate the channel, and such an estimation can be particularly complex if performed in the time domain. It has been shown in [7] that channel estimation can be partitioned into a two-step process if we model the channel as a tapped delay line. That is, we can first determine the channel ray delays, and then we can obtain an estimate of the ray amplitudes. Unfortunately, the ray search has a complexity that grows exponentially with their number. Further, false ray detection may occur in the absence of *a priori* knowledge about the true number of rays. Such a search can be partially simplified under the assumption of the channel to be resolvable [7]–[9]. However, this assumption can translate into deep performance losses in the nonrare event of clusters of nonresolvable rays.

It has also to be emphasized that when common media is shared by multiple users, multiple-access interference (MAI) may arise at the receiver side. In a DS-CDMA system, this is due to the deployment of nonorthogonal codes, or to users that are time asynchronous, or to the presence of channel time dispersion. Assuming a single-user-detection approach, the MAI translates into performance losses, such that some form of multiuser detection is advisable [5], [10].

Motivated by the above considerations, we propose in this paper, a novel FD approach to channel estimation, detection, and MAI cancellation in impulse-radio DS-CDMA systems. It is related to the FD-detection approaches that are used in orthogonal-frequency-division-multiplexing (OFDM) systems

Manuscript received February 16, 2004; revised November 10, 2004; accepted January 9, 2005. The editor coordinating the review of this paper and approving it for publication is A. Molisch. Part of this paper was presented at Wireless Personal Multimedia Communications (WPMC) Symposium 2004, Abano Terme, Italy, September 12–15, 2004. This paper was supported in part by the Italian Ministry of Education, University, and Research (MIUR) under project "Reconfigurable platforms for wideband wireless communications" Prot. RBNE018RFY with the Fund for the Basic Research (FIRB).

The authors are with the Dipartimento di Ingegneria Elettrica, Gestionale e Meccanica, Università di Udine, 33100, Udine, Italy (e-mail: tonello@uniud.it; rinaldo@uniud.it).

Digital Object Identifier 10.1109/TWC.2005.858343

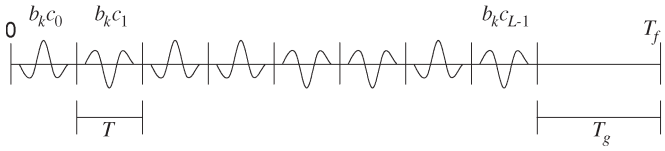

Fig. 1. Frame structure of DS-CDMA with biphase impulse modulation.

[11], and to the FD-equalization technique of cyclically prefixed single-carrier modulation in [12]. Our approach is single-user-based. However, it can include the capability of rejecting the MAI by the exploitation of its correlation in the FD. It has been derived from observation that the maximum-likelihood receiver in the presence of colored-Gaussian noise can be equivalently implemented in the FD. The receiver comprises the following stages. First, we acquire frame synchronization with the desired user. Second, we run a discrete Fourier transform (DFT) on the received frames. Third, we perform FD channel estimation for the desired user via a recursive least-squares (RLS) algorithm [13]. Finally, detection is accomplished in the FD using the estimated channel frequency response. In the presence of MAI, we include the capability of rejecting the interference through the estimation and exploitation of its FD correlation. It is interesting to note that in systems that use multiple receive antennas, cochannel-interference cancellation is possible through the exploitation of the degrees of freedom offered by multiple antennas [14]–[17]. In our FD scheme, MAI suppression is achieved owing to the degrees of freedom afforded both by the spreading codes and the multipath/multiuser channel diversity.

Frame timing is crucial. In this paper, we propose to determine frame timing in the time domain with a two-step procedure that first acquires coarse frame synchronization, then determines fine synchronization by estimating the window where the desired user's signal energy is located.

The paper is organized as follows. In Section II, we describe the principles of the proposed FD-detection approach. For clarity, we first consider the single-user case, then address the multiuser case. In Section III, we describe the practical estimation of the parameters in the FD. In Section IV, we address the frame-synchronization problem. In Section V, we discuss complexity. In Section VI, we report numerical results. Then, the conclusion follows.

II. Frequency-Domain Processing

Herein, we describe the system model, and the proposed FD approach to channel estimation, and detection (see Figs. 1 and 2). We first address the single-user case, then the multiuser case.

A. Single-User Case

In our system model, we assume BPAM [13] such that the signal transmitted by the desired user can be written as

$$s(t) = \sum_k b_k g(t - kT_{\rm f}) \tag{1}$$

where $b_k = \pm 1$ denotes the information bit transmitted in the kth frame, $g(t)$ is the waveform used to convey information, and $T_{\rm f}$ is the bit period (frame duration). We further assume the deployment of direct-sequence spreading [2] to accommodate code-division multiplexing of users as treated in the next section. The waveform (user's signature code) comprises the weighted repetition of $L \geq 1$ narrow pulses (referred to as monocycles), i.e.,

$$g(t) = \sum_{m=0}^{L-1} c_m g_M(t - mT) \tag{2}$$

where $c_m = \pm 1$ are the codeword elements (chips), and T is the chip period (see Fig. 1). We incorporate the differential effects of the transmit, and receive antennas into $g_M(t)$ for ease of notation. We assume $g_M(t)$ to be the second derivative of the Gaussian pulse [1]

$$g_M(t) = \left(1 - \pi \left(\frac{\left(t - \frac{D}{2}\right)}{T_0}\right)^2\right) \exp\left\{-\frac{\pi}{2}\left(\frac{\left(t - \frac{D}{2}\right)}{T_0}\right)^2\right\}. \tag{3}$$

In a typical system design, we can choose $T \geq D$, where $D \approx 5T_0$ is the monocycle pulse duration. We further insert a guard time $T_{\rm g}$ between frames to cope with the channel time dispersion, and eliminate the intersymbol interference (ISI). The frame duration fulfills the relation $T_{\rm f} = LT + T_{\rm g}$, with $T_{\rm g} > T_{\rm ch}$, and $T_{\rm ch}$ being the maximum time dispersion introduced by the channel. If we chose $T \geq D + T_{\rm ch}$, we can also avoid the interpulse interference at the expense of a transmission-rate penalty. However, we do not restrict ourselves to this case.

As shown in Fig. 2, at the receiver side, we first deploy a bandpass front-end filter with impulse response $g_{\rm FE}(t)$ to suppress out band noise and interference. Then, the received signal, in the single-user case, can be written as

$$y(t) = \sum_k b_k g_{\rm EQ}(t - kT_{\rm f}) + \eta(t) \tag{4}$$

where $g_{\rm EQ}(t) = g * h * g_{\rm FE}(t)$ is the equivalent (real) impulse response that comprises the user's waveform filter, the channel $h(t)$, and the front-end filter. The additive noise $\eta(t)$ is assumed to be a stationary zero-mean Gaussian process. Further, in the following, we consider it to be white in the useful signal band. The case of colored noise, however, can be treated as described in Section II-B, where we deal with the MAI. The channel impulse response is assumed to be time invariant over several transmitted frames. Then, it can change in a random fashion. With the popular discrete-multipath model, the channel impulse response can be written as

$$h(t) = \sum_{p=1}^{N_P} \alpha_p \delta(t - \tau_p). \tag{5}$$

As an example, in the numerical results that follow, we assume the tap delays τ_p to belong to a finite time interval, and we

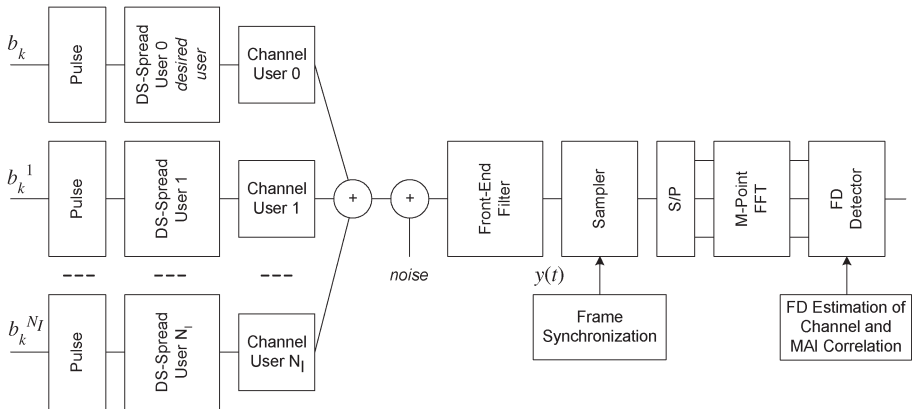

Fig. 2. DS-CDMA impulse-modulated-system model with FD-receiver processing.

assume a $T_{\rm g}$ larger than the duration of the equivalent-channel response. We consider two statistical channel models where the ray delays are either independent and uniformly distributed, or drawn according to a Poisson process. The tap gains α_p are assumed to be real, independent, and equal to $\alpha_p = \chi_p \beta_p$, where $\chi_p = \pm 1$ with equal probability, while β_p are either Rayleigh or log-normal distributed. As proposed in [18], the term χ_p is used to account for the random pulse inversions that are due to reflections, as observed in measurements. The power-delay profile is assumed to be exponential [9]. With these models, the rays can appear in clusters of duration less than D, i.e., the channel is not necessarily resolvable. Indeed, other models are possible as comprehensively described in [18].

Under the above assumptions and with ideal frame synchronization, no ISI arises at the receiver side. Thus, the optimal receiver [6] operates in a symbol-by-symbol fashion by computing the decision metric

$$z_{\rm DM}(kT_{\rm f}) = \int_0^{T_{\rm f}} y_k(t) g_{\rm EQ}(t) dt \tag{6}$$

where $y_k(t) = y(t + kT_{\rm f})$ for $0 \le t < T_{\rm f}$. That is, the decision metric for the kth bit is obtained by correlating the received signal with the real equivalent impulse response $g_{\rm EQ}(t)$, and making a threshold decision, i.e., $\hat{b}_k = \text{sign}\{z_{\rm DM}(kT_{\rm f})\}$. This receiver is referred to as a matched-filter receiver.

If we consider discrete-time processing, the received signal is sampled at the output of the front-end analog filter at a sufficiently high rate to obtain $y_k(nT_{\rm c})$ with $T_{\rm c} = T_{\rm f}/M$. Assuming frame synchronization, the received frame of samples reads

$$y_k(nT_{\rm c}) = b_k g_{\rm EQ}(nT_{\rm c}) + \eta_k(nT_{\rm c}), \quad n = 0, \ldots, M-1 \tag{7}$$

where $\eta_k(nT_{\rm c})$ are zero-mean Gaussian random variables. We assume them to be independent identically distributed (i.i.d.) with variance $N_0/2$ that holds true when the noise in the transmission medium is white and the front-end filter has Nyquist autocorrelation with band $1/T_{\rm c}$. Then, the decision metric is generated as follows

$$z_{\rm DM}(kT_{\rm f}) = \sum_{n=0}^{M-1} T_{\rm c} y_k(nT_{\rm c}) g_{\rm EQ}(nT_{\rm c}). \tag{8}$$

It should be noted that the case of correlated noise samples can also be considered and yields a different decision metric that we describe in the next section. To implement (6) or (8), we need to estimate the channel impulse response. Typically, estimation is performed in the time domain using a training bit sequence. Time-domain channel estimation is complicated by the high number of multipath components exhibited by UWB channels, and by the presence of nonresolvable channel rays, i.e., rays with a relative time delay smaller than the monocycle duration D. Thus, $g_{\rm EQ}(t)$ can be an involved function of the channel, and the transmitted waveform. Maximum-likelihood time-domain channel estimation is described in [7] and [9] under the assumption of a tapped-delay-line channel model. In this paper, we take a different approach by proposing channel estimation, and detection in the FD. To proceed, we can interpret (8) as the cross energy between two discrete time signals that are periodic of $T_{\rm f} = MT_{\rm c}$. By Parseval theorem, we can equivalently obtain the decision metric by operating in the FD as follows

$$z_{\rm DM}(kT_{\rm f}) = \frac{1}{MT_{\rm c}} \sum_{n=0}^{M-1} Y_k(f_n) G_{\rm EQ}^*(f_n) \tag{9}$$

where $Y_k(f_n)$, $G_{\rm EQ}^*(f_n)$ for $f_n = n/(MT_{\rm c})$, $n = 0, \ldots, M-1$, are the M-point DFT outputs of the received frame and of the matched-filter impulse response.[1] The DFT can be efficiently implemented via a fast Fourier transform (FFT). To obtain (9), we need to estimate $G_{\rm EQ}(f_n)$. The attractive feature in (9) is the fact that the matched-filter frequency response at a given frequency depends only on the channel response at that frequency. This greatly simplifies the channel-estimation task,

[1] $(\cdot)^*$ denotes the complex-conjugate operator. The M-point DFT is defined as $A(f_n) = \sum_{k=0}^{M-1} T_{\rm c} a(kT_{\rm c}) {\rm e}^{-j2\pi k T_{\rm c} f_n}$ with $f_n = n/(MT_{\rm c})$, $n = 0, \ldots, M-1$.

as we will describe in detail in Section III. By exploiting the Hermitian symmetry of $G_{\mathrm{EQ}}(f_n)$, the estimation can be carried out only over $M/2$ frequency bins. A further simplification is obtained by observing that the Fourier transform of the desired user's waveform at frequency f_n can be written as

$$G(f_n) = G_M(f_n) \sum_{m=0}^{L-1} c_m \mathrm{e}^{-j2\pi f_n mT}. \tag{10}$$

If we deploy a monocycle that has a frequency-concentrated response, as the Gaussian pulse in (3), we can assume that $G_M(f_n) \approx 0$ for, say, $f_n > 2/D$. Therefore, relevant signal energy is present only in a small number of frequency bins, and consequently, channel estimation can be performed only over this fraction of bins. If $D = K_D T_{\mathrm{c}}$, an estimate of the number of such subchannels is $2M/K_D$.

Another interesting characteristic of the FD-channel-estimation approach is that no restrictive assumption about the channel-impulse-response statistics has been made. Indeed, it has to be pointed out that the FD approach requires frame synchronization. We will propose a practical solution to this problem in Section IV.

B. Multiuser Case

In the presence of N_{I} other users (interferers), the received signal can be rewritten as

$$y(t) = \sum_k b_k g_{\mathrm{EQ}}(t - kT_{\mathrm{f}}) + i(t) + \eta(t)$$

$$i(t) = \sum_{u=1}^{N_{\mathrm{I}}} \sum_k b_k^u g_{\mathrm{EQ}}^u(t - kT_{\mathrm{f}} - \Delta_u). \tag{11}$$

The uth user's equivalent impulse response is denoted as $g_{\mathrm{EQ}}^u(t) = g^u * h^u * g_{\mathrm{FE}}(t)$, while b_k^u are the information bits of user u with an alphabet equal to ± 1, and Δ_u denotes the time delay of user u with respect to the desired user's frame timing. The equivalent impulse response comprises the convolution of the uth user's transmission waveform (signature code) with its channel impulse response and the front-end filter. The uth user's transmission waveform is obtained as in (2) by the assignment of a binary codeword with elements c_m^u, $m = 0, \ldots, L-1$, that have an alphabet of ± 1. We add a guard time T_{g} to each user's frame, and we can choose the codewords to be either orthogonal or random (pseudonoise). The users have equal-duration frames and code lengths. They experience independent channels that we assume to introduce identical maximum time dispersion.

Also in this scenario, we pursue a single-user detection approach, i.e., the receiver wants to detect the desired user's bits b_k only (see Fig. 2). For this purpose, we proceed through the following steps. We acquire frame synchronization with the desired user; we estimate its channel equivalent response in the FD, and finally, we run the matched-filtering operation (9). If the noise is white, the users are synchronous, the channels are nondispersive, the codes are orthogonal, and the chip period is larger than the monocycle duration, the matched-filter receiver or equivalently its FD implementation is optimal, since neither ISI nor MAI is exhibited at the matched-filter output. In practicality, MAI is present due to the deployment of nonorthogonal spreading codes, the presence of asynchronous users, and channel dispersion [10].

Now, our goal is to operate in the FD by introducing an appropriate modification of (9) that takes into account the presence of the MAI. We start by collecting M samples at the output of the analog front-end filter in correspondence with the kth frame of the desired user. We deploy an M-point DFT, obtaining in the presence of MAI

$$Y_k(f_n) = b_k G_{\mathrm{EQ}}(f_n) + I_k(f_n) + N_k(f_n), \quad n = 0, \ldots, M-1 \tag{12}$$

where $N_k(f_n)$ is the DFT of the noise samples $\eta_k(nT_{\mathrm{c}})$, while $I_k(f_n)$ is the DFT of the MAI term $i_k(nT_{\mathrm{c}})$, and $G_{\mathrm{EQ}}(f_n)$ is the DFT of $g_{\mathrm{EQ}}(nT_{\mathrm{c}})$. No ISI is present for the desired user assuming perfect frame timing and a sufficiently long guard time. The MAI additive term in the presence of asynchronous, or synchronous users, respectively, reads

$$I_k(f_n)_{\mathrm{async}} = \sum_{u=1}^{N_{\mathrm{I}}} \sum_{m=0}^{1} b_{k-m}^u G_{\mathrm{EQ}}^u(f_n, m) \tag{13}$$

$$I_k(f_n)_{\mathrm{sync}} = \sum_{u=1}^{N_{\mathrm{I}}} b_k^u G_{\mathrm{EQ}}^u(f_n, 0) \tag{14}$$

where $G_{\mathrm{EQ}}^u(f_n, m)$ is a function of the users' time delay, transmitted waveform, and channel. Details are reported in the Appendix A. Note that in the asynchronous case, two information bits per user may cause interference, while in the synchronous case, only one bit generates interference.

To derive the proposed receiver, we model the noise plus interference $z(kMT_{\mathrm{c}} + nT_{\mathrm{c}}) = z_k(nT_{\mathrm{c}}) = i_k(nT_{\mathrm{c}}) + \eta_k(nT_{\mathrm{c}})$ with a discrete-time colored-Gaussian process with correlation function[2] $r(nT_{\mathrm{c}}, lT_{\mathrm{c}}) = E[z(nT_{\mathrm{c}})z(lT_{\mathrm{c}})]$. Then, assuming the transmitted bits of all users to be i.i.d. and equally likely, the DFT outputs $Z_k(f_n) = I_k(f_n) + N_k(f_n)$ are complex Gaussian with zero mean. The impairment multivariate process $\mathbf{Z}_k$ defined as $\mathbf{Z}_k = [Z_k(f_0) \ \cdots \ Z_k(f_{M-1})]^{\mathrm{T}}$, has a time–frequency correlation matrix equal to[3]

$$\mathbf{R}(k,m) = E\left[\mathbf{Z}_k \mathbf{Z}_m^{\dagger}\right] = \mathbf{F}\mathbf{K}(k,m)\mathbf{F}^{\dagger} \tag{15}$$

where $\mathbf{K}(k,m)$ is the $M \times M$ matrix with entries $r(kM + n, mM + l)$ for $n, l = 0, \ldots, M-1$, and $\mathbf{F}$ is the M-point DFT orthonormal matrix. With uncorrelated thermal-noise samples, $\mathbf{R}(k,m) = 0$ for $|m-k| > 1$ in the asynchronous

[2] $E[\cdot]$ denotes the expectation operator.

[3] $(\cdot)^{\mathrm{T}}$ denotes the transpose operator. $(\cdot)^{\dagger}$ denotes the conjugate-and-transpose operator.

MAI case, while $\mathbf{R}(k,m)=0$ for $|m-k|>0$ in the synchronous case (see Appendix A).

Now, let us collect the elements of $Y_k(f_n)$, and of $G_{\rm EQ}(f_n)$, in the vectors $\mathbf{Y}_k=[Y_k(f_0)\cdots Y_k(f_{M-1})]^{\rm T}$ and $G_{\rm EQ}=[G_{\rm EQ}(f_0)\cdots G_{\rm EQ}(f_{M-1})]^{\rm T}$. Then, we show in Appendix B that under the above colored-Gaussian-impairment model, the maximum-likelihood receiver can be equivalently implemented in the FD by searching the sequence of transmitted bits $\{\hat{b}_k\}$ (belonging to the desired user) that maximizes the log-likelihood function[4]

$$\Lambda\left(\{\hat{b}_k\}\right)=-\sum_{k=-\infty}^{\infty}\sum_{m=-\infty}^{\infty}[\mathbf{Y}_k-\hat{b}_k\mathbf{G}_{\rm EQ}]^{\dagger}\times\mathbf{R}^{-1}(k,m)[\mathbf{Y}_m-\hat{b}_m\mathbf{G}_{\rm EQ}]. \quad (16)$$

In order to simplify the algorithm complexity, we neglect the temporal correlation of the interference (MAI+noise) vector $\mathbf{Z}_k$, i.e., we assume $\mathbf{R}(k,m)=0$ for $k\neq m$. Indeed, the MAI correlation across frames is zero only for the synchronous case. Then, by dropping the terms that do not depend on the information bit of the desired user, the log-likelihood function simplifies to

$$\Lambda(\hat{b}_k)\sim\hat{b}_k{\rm Re}\left\{\mathbf{G}_{\rm EQ}^{\dagger}\mathbf{R}^{-1}(k,k)\mathbf{Y}_k\right\}. \quad (17)$$

Therefore, according to (17), the FD receiver operates on a frame-by-frame basis, and it exploits the frequency correlation of the MAI. The computation in (17) can be interpreted as the result of matching the frequency response of the kth frame with $\mathbf{G}_{\rm EQ}^{\dagger}\mathbf{R}^{-1}(k,k)$ to obtain the interference-cancellation metric

$$z_{\rm IC}(kT_{\rm f})=\mathbf{G}_{\rm EQ}^{\dagger}\mathbf{R}^{-1}(k,k)\mathbf{Y}_k. \quad (18)$$

Then, we make a decision on the transmitted bit looking at the sign of (18). Note that (18) is real, given that the quantities involved have Hermitian symmetry.

The main idea behind the algorithm above is to perform interference cancellation in the FD via decorrelation of the MAI. Similar, in spirit, approaches have been proposed for cochannel interference cancellation in systems that deploy receive-antenna arrays and use spatial-interference decorrelation through combination of the received antenna signals [14]–[17]. Herein, interference suppression is achieved owing to the degrees of freedom offered both by the spreading codes and the multipath/multiuser channel diversity, as compared with the degrees of freedom afforded by multiple antennas.

In the absence of MAI and with uncorrelated noise samples, the correlation matrix is diagonal with diagonal elements equal to the noise variance. In such a case, the detection metric collapses to (9). Further, both the metric (16) and (18) can account for the presence of correlated noise samples.

From a practical implementation perspective, we need to estimate both the desired user's channel frequency response, and the interference (impairment) correlation matrix. We assume the correlation matrix to be full rank, otherwise pseudoinverse techniques can be used. It is interesting to note that a further simplification of the metric (18) is possible if we process only the frequency bins for which $|G(f_n)|$ is sufficiently large. In this case, we estimate the desired user-channel frequency response and the interference correlation matrix only over this subset of frequency bins.

III. Frequency-Domain Parameter Estimation

In this section, we address the problem of estimating the frequency response of the desired user channel, and the interference (MAI+noise) correlation matrix in (18). We assume the deployment of a training sequence of known bits. To keep it at low complexity, we perform estimation in a two-step procedure. First, we estimate the desired user's channel. Then, we estimate the impairment-correlation matrix. We implicitly assume the users' channel and delay to be static, and the MAI plus noise vector $\mathbf{Z}_k$ to be stationary over the transmission of several frames, such that we can denote its correlation matrix with $\mathbf{R}(k,k)=\hat{\mathbf{R}}$. This holds true, for instance, assuming users with identical frame duration and spreading code length. However, we point out that during the detection stage, the algorithms that we describe allow the performance of adaptation to a channel and MAI variations in a data-decision-directed mode.

A. RLS Frequency-Domain Estimation of the Desired User's Channel

Under the assumption of deploying a training sequence of N bits, the M-bins channel frequency response can be obtained via a recursive least mean-square estimator [12], [13]. The estimator operates independently over the frequency bins by recursively updating the channel estimates. We herein consider the RLS algorithm, which, in this scenario, is slightly more complex than the LMS algorithm but exhibits much-superior convergence properties [13]. We start by approximating the frequency response of the equivalent channel of the desired user as follows

$$\hat{G}_{\rm EQ}(f_n)\approx G(f_n)\hat{H}(f_n),\quad n=0,\ldots,M-1 \quad (19)$$

where $G(f_n)$ denotes the M-point DFT of the desired user's waveform (at frequency f_n), and $\hat{H}(f_n)$ denotes the estimate of the channel frequency response that includes the effect of the front-end filter. Then, with some simple modifications to the one-tap RLS algorithm, we compute the M-frequency-bins channel estimates as follows

$$\hat{H}_i(f_n)=\hat{H}_{i-1}(f_n)+e_i(f_n)K_i(f_n) \quad (20)$$

[4]Let $\mathbf{R}$ be the matrix whose $M\times M$ block of indices (k,m) is $\mathbf{R}(k,m)$ and let $\mathbf{R}^{-1}$ be its inverse. Then, $\mathbf{R}^{-1}(k,m)$ denotes the $M\times M$ block of indices (k,m) of $\mathbf{R}^{-1}$. If $\mathbf{R}$ is block diagonal, e.g., when we neglect the impairment correlation across frames, $\mathbf{R}^{-1}(k,k)=(\mathbf{R}(k,k))^{-1}$.

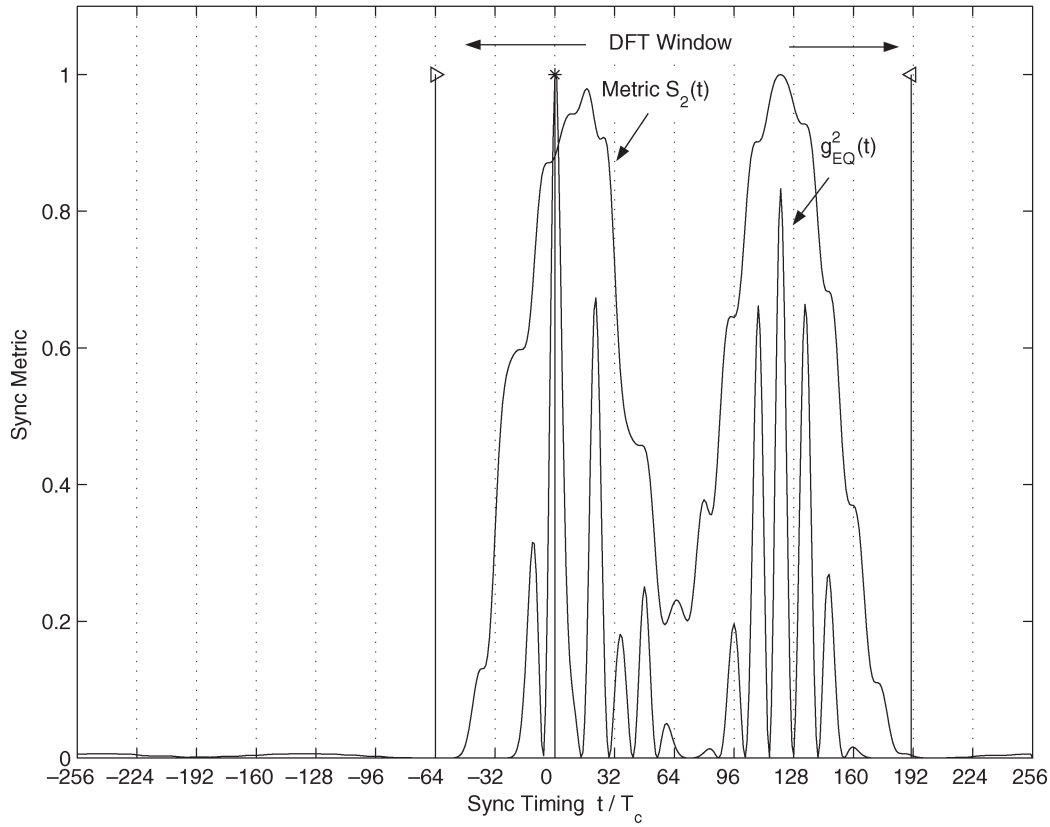

Fig. 3. Example of normalized synchronization metric in the absence of noise.

where the error for the ith frame and nth frequency bin is defined as

$$e_i(f_n) = b_i Y_i(f_n) - \hat{H}_{i-1}(f_n) G(f_n) \tag{21}$$

and b_i, $i = 0, \ldots, N-1$, is the known training bit transmitted in the ith frame by the desired user. The Kalman gain is updated according to

$$\begin{aligned} K_i(f_n) &= P_{i-1}(f_n) G^*(f_n) \left(\lambda + P_{i-1}(f_n) |G(f_n)|^2 \right)^{-1} \\ P_i(f_n) &= \lambda^{-1} \left(1 - K_i(f_n) G(f_n) \right) P_{i-1}(f_n). \end{aligned} \tag{22}$$

We start with $P_0(f_n) = 1/d$, and we choose in all numerical examples that follow, $d = 0.01$ and $\lambda = 0.999$.

B. Estimation of the Frequency-Domain Interference Correlation Matrix

Once we have computed the desired user's FD channel estimate $\hat{\mathbf{G}}_{\mathrm{EQ}}$, we compute an estimate of the interference-correlation matrix $\hat{\mathbf{R}}$. Let us define the error vector in correspondence with the ith frame as $\hat{\mathbf{E}}_i = b_i \mathbf{Y}_i - \hat{\mathbf{G}}_{\mathrm{EQ}}$, where $\{b_i\}$, $i = 0, \ldots, N-1$, is the sequence of known training bits of the desired user. Then, we estimate the correlation matrix [14], [15] as

$$\hat{\mathbf{R}} = \frac{1}{N} \sum_{i=0}^{N-1} \hat{\mathbf{E}}_i \hat{\mathbf{E}}_i^{\dagger}. \tag{23}$$

Alternatively, it can be recursively estimated according to $\hat{\mathbf{R}}_i = \beta \hat{\mathbf{R}}_{i-1} + (1-\beta) \hat{\mathbf{E}}_i \hat{\mathbf{E}}_i^{\dagger}$, for $i = 0, \ldots, N-1$, using a forgetting factor $0 < \beta < 1$.

In the absence of MAI and with white noise only, the correlation matrix is diagonal, with diagonal elements equal to the noise variance. In such conditions, the performance of the canceling algorithm that performs practical estimation of the correlation matrix may be lower than the performance of the noncanceling algorithm. Thus, to introduce a tradeoff between the effects of noise, and the effects of the MAI, we can adjust the correlation matrix as $\hat{\mathbf{R}} = (1-\rho)\hat{\mathbf{R}} + \rho \sigma_N^2 \mathbf{I}$ with $\rho \leq 1$, and $\mathbf{I}$ equal to the identity matrix. This technique is referred to as diagonal loading or eigenvalues shifting [21]. The noise variance σ_N^2 can be set to a fixed value according to the range of operating signal-to-noise ratios.

IV. Frame Synchronization

In this section, we describe a frame-synchronization scheme that operates in the time domain. Again, we assume to send a training bit sequence $\{b_i\}$ of length N. The method is divided in two steps. First, we acquire coarse synchronization with the desired user's training sequence. Second, we acquire fine timing. That is, we exactly determine where the desired user's frame starts and ends. The scheme is by no means optimal, but it has been chosen as a good tradeoff between performance and complexity. Recall that the knowledge of the frame timing is needed for implementing the FD channel estimator that we have described before. In Fig. 3, we show an example of the synchronization metrics that we define in what follows.

A. First Step—Coarse Timing

Coarse timing is obtained by locking on the time instant where the channel exhibits the highest energy. We refer to it as the highest energy-channel tap (Fig. 3). We assume a sampling resolution equal to T_c. Then, the training-sequence coarse starting epoch $t_1 = \hat{p}_1 T_c$ is determined as follows

$$\hat{p}_1 = \arg\max_{p \in \mathbb{Z}} \left\{ |S_1(p)|^2 \right\} \tag{24}$$

$$S_1(p) = \frac{1}{N} \sum_{i=0}^{N-1} b_i y(pT_c + iMT_c). \tag{25}$$

The metric (24)–(25) derives from the observation that in correspondence with the training sequence (without noise), the frame signals are identical besides the sign flip imposed by the training bits.

B. Second Step—Fine Timing

Once we have locked into the highest energy-channel tap, i.e., we have determined $t_1 = \hat{p}_1 T_c$, we basically have a coarse knowledge of where the frame that corresponds to the first known training bit, is located. We now need to refine the synchronization by establishing exactly where the frame is located around the highest energy-channel tap (Fig. 3). We do not make any assumption on the channel, i.e., we do not assume it to have, for instance, a single- or double-sided exponential power-delay profile. The fine synchronization strategy that we propose in this paper is based on the idea of looking at the received energy content of windows of duration MT_c. The starting epoch of a given window falls in the interval $[(-M + \hat{p}_1)T_c, (M + \hat{p}_1)T_c]$. To keep the complexity at moderate levels, we down sample that interval by a factor M_w, so that the frame starting epoch is taken to be $t_2 = \hat{p}_1 T_c + \hat{p}_2 M_w T_c$ for a given $\hat{p}_2 \in \{-M/M_w, \ldots, M/M_w\}$. The integer $\hat{p}_2$ is determined via the following maximization

$$\hat{p}_2 = \arg\max_{p \in \left\{-\frac{M}{M_w}, \ldots, \frac{M}{M_w}\right\}} \sum_{i=0}^{\frac{M}{M_w}-2} S_2(pM_w + iM_w) \tag{26}$$

$$S_2(p) = \frac{1}{2M_w} \sum_{k=-M_w}^{M_w-1} |S_1(p + \hat{p}_1 + k)|^2 . \tag{27}$$

Note that (27) yields an estimation of the received energy in a window of duration $2M_w$ that is centered at time instant $pT_c + \hat{p}_1 T_c$. Overall, (26) corresponds to computing the received energy in a frame of duration MT_c, and to smoothing by one half the energy content of the two windows of M_w samples at the beginning and the end of the frame itself.

V. Considerations on Complexity

The complexity of the proposed estimation and detection approach is a function of the system-design parameters in terms of occupied bandwidth, and frame duration (symbol rate). Typically, the frame duration is much larger than the pulse duration. Nevertheless, it has to be noted that the sampling-rate requirement can be high depending on the pulse bandwidth. Intrinsically, this is a source of complexity for any UWB system. In our approach, the number of samples per frame that we need to process, and consequently, the number of DFT points, is directly related to the channel-resolvability capability of the receiver. The higher is the desired time resolution for channel estimation, the higher the number of samples (and DFT points) per frame we need to process. If we do not possess any *a priori* knowledge on the channel (besides the assumption of it to be shorter than the frame duration) we need to deploy the DFT over the whole frame. However, if the channel is sparse, and manifests itself as a number of resolvable clusters, we can simplify complexity by deploying a pruned DFT. That is, we can set to zero the input samples that do not carry useful signal energy. As an example, suppose that the equivalent impulse response spans the first half of the frame only. Then, to collect the signal energy, we do not need to use the samples that fall in the second half of the frame. This has an advantage not only in terms of complexity but also in terms of performance, because the second half of the frame carries only noise. Practically speaking, if for instance, $S_2(pM_w) < E_t$ for a given p, and for a certain threshold E_t, we can set to zero the $2M_w$ received samples that are used to compute $S_2(pM_w)$ according to (27).

We point out that in certain conditions it is possible, and convenient, to deploy parameter estimation in the FD while detecting in the time domain. As an example, consider the case when the channel exhibits a small number of resolvable rays K. Then, the time-domain Rake receiver only needs to combine K fingers [6], [8]. Following our approach, we can first perform channel estimation in the FD. Then, we can compute the Rake fingers (delays and amplitudes) via an inverse DFT. Finally, detection can be performed in the time domain by combining the Rake fingers at low symbol rate. Indeed, since no *a priori* knowledge of the channel is available, we need to run channel estimation at high sampling rate. However, during training, it is possible to lower the requirements on the analog-to-digital-converter sampling rate with the approach that has been proposed in [8]. It is based on the idea of repeating K_R times the training sequence of length N, and using a polyphase sampling filter bank of size K. Each sampler (one per finger) works at symbol rate $1/(MT_c)$ with $M = K_R K$, but the initial time of the sampler of index $l = 0, \ldots, K-1$ is adjusted to $t_{l,i} = lK_R T_c + iT_c$, in correspondence with the $i = 0, \ldots, K_R - 1$ training-sequence repetition. Thus, after NK_R frames, we have available NM samples with a resolution equal to T_c. In combination or as an alternative to this technique, we can also resort to conventional interpolation techniques as suggested in [9].

VI. Performance Evaluation

To assess the performance of the proposed algorithm, we first consider the single-user case, then the multiuser case. In the simulations, we assume a training sequence of length N bits, followed by 1000 information bits that are used to estimate the

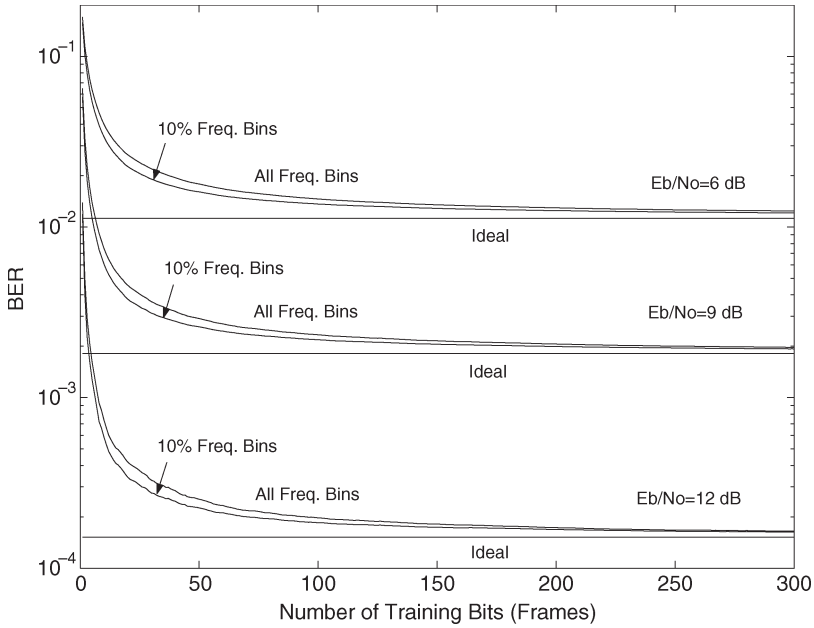

Fig. 4. BER performance as a function of the number of training bits (frames) for a fixed average signal-to-noise ratio in the single-user case with no DS spreading and perfect-frame synchronization.

bit error rate (BER) for a given channel realization. Averaging over at least 1000 channel realizations is then performed. The sampling period $T_{\rm c}$ is taken as the time unit, and we use three statistical-channel models with unit average power for the response (5).

- Channel A: It has $N_P = 10$ rays that have uniform delay distribution within $[0, T_{\rm f} - D)$, and a Rayleigh amplitude with an equally likely sign flip. $T_{\rm f}$ is the frame duration, while D is the monocycle duration. The rays have average power $\Omega_p = E[\alpha_p^2] \sim {\rm e}^{-\tau_p/D}$, $p = 0, \ldots, N_P - 1$.
- Channel B: The ray delays belong to the interval $[0, T_{\rm f} - D)$ and are drawn from a Poisson process with mean arrival rate Λ/D. The ray amplitudes are log-normal distributed with an equally likely sign flip. The first ray is fixed at time instant 0. The rays have power $\Omega_p \sim {\rm e}^{-\tau_p/(\Gamma D)}$ for a given decay factor Γ, and mean $E[\alpha_p] = 0.5\sqrt{\Omega_p \pi}$. Note that Λ represents the mean number of rays per monocycle in the underlying arrival Poisson process.
- Channel C: It is like channel A with $N_P = 5$ rays in $[0, T_{\rm f} - 8D)$, with power $\Omega_p \sim {\rm e}^{-\tau_p/(1.5D)}$.

A. Single-User Case

In the single-user case, we assume no spreading, i.e., we deploy a length $L = 1$ code, and we assume the deployment of a guard time that is sufficiently long to absorb the channel time dispersion.

1) Convergence Performance of the Channel Estimator: We evaluate the performance of the channel estimator in terms of BER assuming perfect frame timing (see Fig. 4). The simulation assumes the channel A model with $T_{\rm f} = MT_{\rm c}$, $M = 256$, $D = 63T_{\rm c}$. With this model, rays can appear in clusters of duration smaller than the pulse duration. With practical channel estimation, the decision statistics become

$$\hat{z}_{\rm DM}(kT_{\rm f}) = \frac{b_k}{MT_{\rm c}} \sum_{n=0}^{M-1} G_{\rm EQ}(f_n)\hat{G}^*_{\rm EQ}(f_n) + \frac{1}{MT_{\rm c}} \sum_{n=0}^{M-1} N_k(f_n)\hat{G}^*_{\rm EQ}(f_n). \quad (28)$$

We assume the noise in the medium to be white and a unit-energy front-end filter that has Nyquist autocorrelation, such that $\eta_k(nT_{\rm c})$ are i.i.d. Gaussian random variables with zero mean, and variance $N_0/2$. Therefore, the BER conditioned on a given channel estimate is [13]

$${\rm BER}(\hat{G}_{\rm EQ}) = Q\left(\frac{\left| \sum_{n=0}^{M-1} G_{\rm EQ}(f_n)\hat{G}^*_{\rm EQ}(f_n) \right|}{\sqrt{\frac{MT_{\rm c}^2 N_0}{2} \sum_{n=0}^{M-1} \left| \hat{G}_{\rm EQ}(f_n) \right|^2}} \right). \quad (29)$$

With ideal estimates, the conditional BER is obtained by setting $\hat{G}_{\rm EQ}(f_n) = G_{\rm EQ}(f_n)$. The average BER is obtained via Monte Carlo simulation. It is shown in Fig. 4 for a fixed value of the average signal-to-noise ratio $E_{\rm b}/N_0$, with $E_{\rm b} = E[\int g^2_{\rm EQ}(t)dt]$, and as a function of the number of iterations (length of training sequence, or number of frames). As the plot shows, the convergence of the practical estimator to the performance that is achieved with ideal matched filtering is fast. Although the order of 100 iterations may seem large, recall that herein, the equivalent-channel impulse response can span an entire frame of $M = 256$ samples. We report both the performance that is obtained when we combine all frequency bins (curves labeled

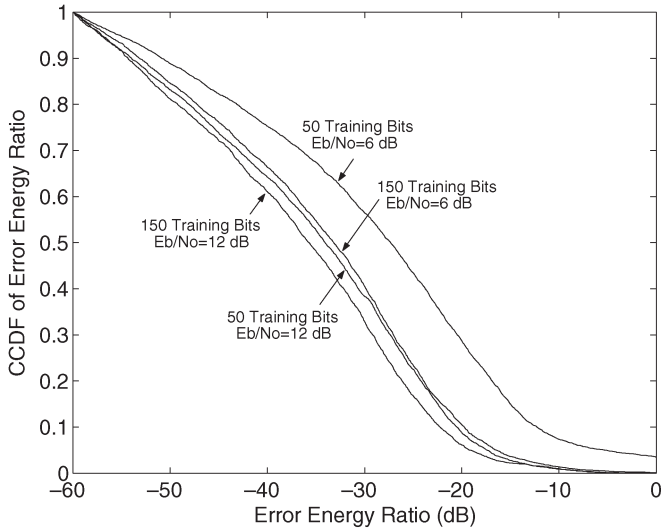

Fig. 5. Complementary cumulative-distribution function of synchronization error-energy ratio.

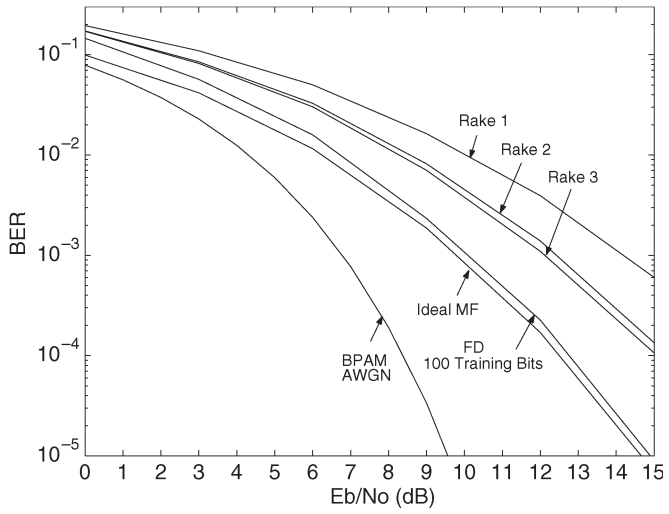

Fig. 6. Average BER performance in a single-user scenario (without DS spreading) with ideal matched filtering, with practical frame synchronization and FD channel estimation, and with a practical Rake receiver with up to three fingers.

with "All Freq. Bins" in Fig. 4), and the performance that is obtained when we combine only the bins for which $|G(f_n)| \geq 0.1 \times \max_k\{|G(f_k)|\}$ (curves labeled with "10% Freq. Bins"). We have found that with ideal matched filtering, there is no appreciable performance difference. However, with practical estimation, we actually improve performance. This is because the estimation over frequency bins that have small signal energy is poor and can negatively affect the BER performance. We point out that for the "10% Freq. Bins" curves, channel estimation is performed only over 17 bins out of 256 (also exploiting the Hermitian symmetry).

2) Performance of the Frame Synchronizer: To characterize the performance of the frame synchronizer, a significant parameter is the ratio of the energy we miss within a frame over the overall energy (referred to as the error-energy ratio). If Δ_0 denotes the error in the estimated frame start-time, and $g_{\rm EQ}(t)$ is the true equivalent-channel impulse response, the error-energy ratio is defined as

$$E_{\rm err}(\Delta_0) = 1 - \frac{\int_{\Delta_0}^{\Delta_0+T_f} g_{\rm EQ}^2(t)dt}{\int_0^{T_f} g_{\rm EQ}^2(t)dt}. \qquad (30)$$

The error-energy ratio is zero when we are perfectly synchronized, while it is one when we miss a whole frame.

In Fig. 5, we report the complementary cumulative distribution function of $E_{\rm err}(\Delta_0)$ obtained assuming 10 000 channel realizations. The same parameters and channel model of Fig. 4 are used. Even with 50 training bits, the probability of having a significant error-energy ratio is small. The performance improvement with a training sequence of length 150 is sensible for the low $E_{\rm b}/N_0$ values.

3) Performance of the Overall Algorithm: The performance of the overall algorithm that combines frame synchronization and channel estimation is shown in Fig. 6. We deploy 100 training bits. We use the same parameters and the channel model A as for Figs. 4 and 5. The proposed FD algorithm has a performance close to the ideal matched filter. Further, note that we only combine (process) the frequency bins that have an amplitude above 10% the maximum of $|G(f_n)|$. We also report the performance that is obtained with the time-domain Rake receiver that combines one, two, or three resolvable rays. The Rake receiver is implemented according to the algorithm that is described in [7, Appendix], in particular [7, eqs. (31) and (32)], assuming 100 training bits. This algorithm is based on the assumption of a resolvable channel. Nevertheless, the procedure that exhaustively searches the ray delays is quite complex. Further, the performance penalty is significant, since it is incapable of capturing the channel energy that is associated to clusters of rays of duration smaller than D.

We emphasize that the proposed FD receiver does not rely on a particular statistical-channel model. However, its benefit compared to the Rake receiver in the single-user case is a function of how resolvable the channel is. To show this point, we report in Fig. 7, the BER performance for channel model B. In particular in Fig. 7(a), we fix the $E_{\rm b}/N_0$ to 8 dB and we plot the BER as a function of the average number of rays per monocycle Λ, fixing $\Gamma = 4.75$. In Fig. 7(b), we plot the BER as a function of the normalized decay factor Γ, fixing $\Lambda = 4.75$. Furthermore, the simulation assumes $T_{\rm f} = MT_{\rm c}$, $M = 256$, $D = 25T_{\rm c}$. The channel can span about nine monocycles. As a comparison, we plot the performance of the Rake receiver that combines up to eight resolvable fingers, i.e., spaced by at least D. To allow for practical implementation, the ray search is independently done as described in [9]: we look for the resolvable maxima at the output of the front-end filter that is matched to the monocycle. This is because the optimal joint ray-search algorithm in [7] is prohibitively high. This Rake receiver is very simple although suboptimal. Now, Fig. 7(a) shows that as the average number of rays per monocycle increases, the performance of the FD channel estimator increases, while the Rake receiver actually worsens. This is because the Rake receiver is not capable of capturing all the channel energy and

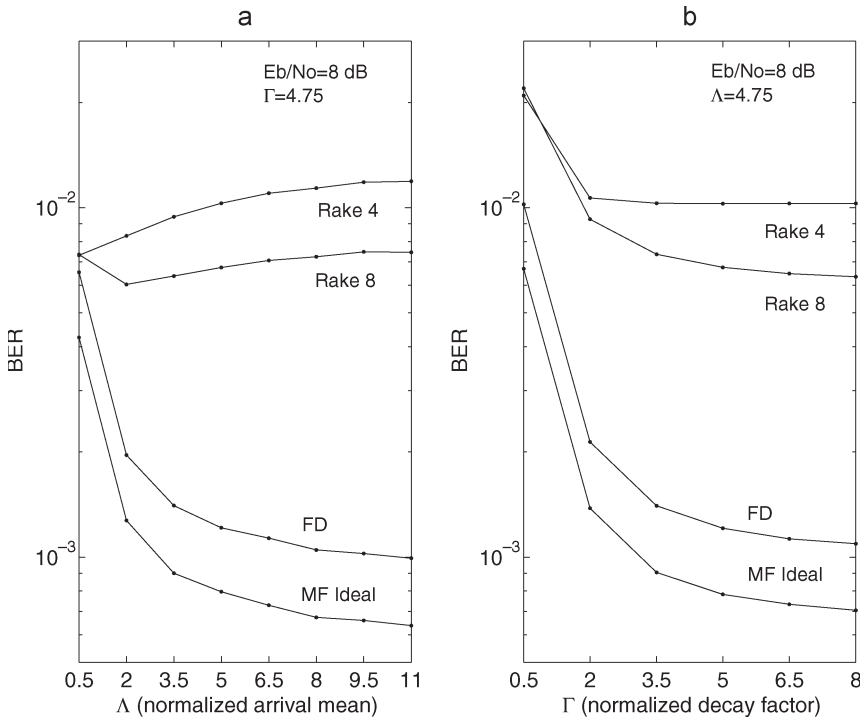

Fig. 7. Average BER performance in a single-user scenario (without DS spreading and with ideal frame synchronization) (a) as a function of the normalized average number of rays per monocycle and (b) as a function of the normalized decay factor (delay spread).

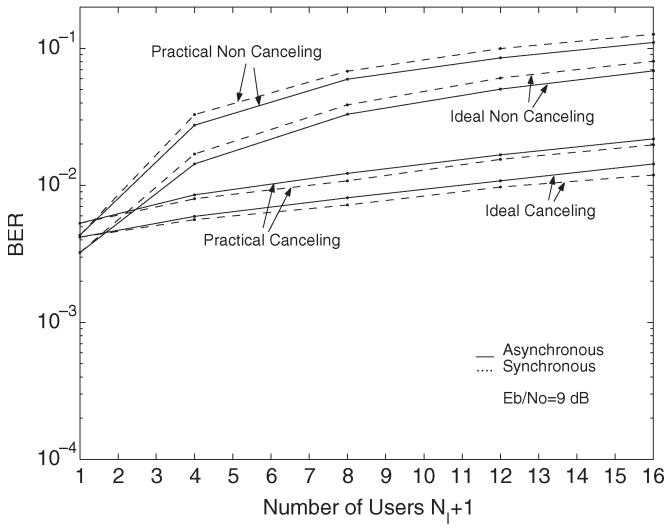

Fig. 8. Average BER performance in a multiuser scenario with synchronous and asynchronous users. Equal-power users with $E_{\rm b}/N_0 = 9$ dB. Random spreading codes of length 8. Curves labeled "ideal" assume ideal channel knowledge and frame timing. Curves labeled "practical" assume practical frame synchronization and channel estimation with 150 training bits.

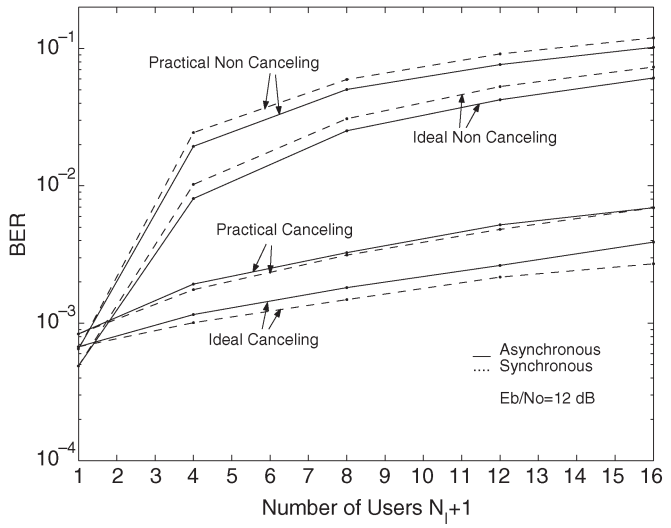

Fig. 9. Average BER performance in a multiuser scenario with synchronous and asynchronous users. Equal-power users with $E_{\rm b}/N_0 = 12$ dB. Random spreading codes of length 8. Curves labeled "ideal" assume ideal channel knowledge and frame timing. Curves labeled "practical" assume practical frame synchronization and channel estimation with 150 training bits.

fully exploiting diversity. For also the same reason in Fig. 7(b), the Rake receiver performs worse than the FD algorithm as the decay factor (delay spread) increases.

B. Multiuser Case

The performance of the proposed algorithm in a multiuser scenario is shown in Figs. 8 and 9. We deploy independent random (pseudonoise) short codes of length $L = 8$ for all users. This allows us to keep the simulation runtime within moderate values. Longer codes shall yield improved performance. The chip period is set to $T = D = 25T_{\rm c}$. The frame has length $T_{\rm f} = 256T_{\rm c}$ for all users. The training sequence has length $N = 150$ bits. The users experience independent channels according to the model C described before. Both the synchronous case (dashed curves) and the asynchronous-users case (solid curves) are considered. For the asynchronous case, the users' time delays are independent and uniformly distributed within

a frame interval. The average signal-to-noise ratio is set to $E_{\rm b}/N_0 = 9$ dB in Fig. 8, while it is set to 12 dB in Fig. 9. Users have equal average bit energy $E_{\rm b}$.

The figures show that a sensible performance degradation arises in the presence of multiple users if we deploy the algorithm that does not cancel the MAI [correlation receiver of Section II-A with the decision metric (9)]. This also happens in the synchronous-users case due to the interchip interference generated by the dispersive channel. Note that we also simulate an overloaded-system scenario, i.e., we allocate more than $L = 8$ users. Curves labeled with ideal have been obtained assuming ideal knowledge of the channel and frame timing of the desired user, while the curves labeled with practical have been obtained by estimating both the frame timing and the channel (with the FD RLS algorithm).

Performance can be significantly improved by deploying the proposed FD MAI canceling algorithm of Section II-B with the decision metric (18). In both the ideal and the practical case, the interference correlation matrix has been estimated over the training sequence of length 150 bits according to (23). Diagonal loading with a loading factor of 0.5 has been used. This is for improving the performance with a small number of users, i.e., when performance is dominated by the noise rather than by the MAI. Furthermore, we combine only the frequency bins that have an amplitude above 10% of the maximum of $|G(f_n)|$. In our simulations, this resulted to, at most, 82 overall frequency bins.

The figures show that the performance of the algorithm that does not cancel the MAI rapidly decreases as the number of users increases as a result of the decreasing signal-to-noise-plus-interference ratio. On the other hand, the canceling algorithm performs well, and exhibits a much flatter performance-curve slope with both ideal and practical channel estimation. We point out that the training parameters ($d = 0.01,\ \lambda = 0.999,\ \rho = 0.5$) have been kept fixed for all scenarios. Indeed, further improvements are expected by deploying longer training sequences, and by optimizing the parameters. A possible method (although not shown) to increase the performance of the channel estimator and the MAI correlation estimator, is to deploy a decision-aided approach, i.e., we can update the estimates as bit decisions are made that would also allow the tracking of MAI/channel variations. Finally, we point out that the loss of performance that is due to the practical frame synchronizer is also small in the presence of MAI.

VII. Conclusion

We have considered the synchronization, channel estimation, and detection problem in biphase impulse-radio systems with DS-CDMA. We have proposed carrying out channel estimation for the desired user via an RLS algorithm in the FD. Frame synchronization is acquired in the time domain. It is based on the following steps. First, locking on to the highest energy-channel tap. Then, fine frame timing is obtained by comparing the energy content of time windows that lay around the main tap. Detection can be performed in the FD. In the presence of MAI, the FD-detection approach allows for the inclusion of the capability of canceling the MAI. A simple solution has been proposed, and it is based on the exploitation of the MAI-plus-noise correlation in the FD. Several practical aspects have been considered as the estimation of the interference-correlation matrix. An interesting aspect of the proposed channel-estimation approach is its moderate complexity compared to the optimal maximum-likelihood time-domain channel estimator [7] that needs to run an exhaustive ray search with exponential complexity in the number of rays. Our scheme requires an FFT, however, RLS training is performed only over a small fraction of the overall number of frequency bins. In fact, only the sufficiently high energy-frequency bins contribute to the detection metric, and need to be processed. Several numerical results have been reported and demonstrate that the proposed approach exhibits fast convergence and high performance with or without synchronous/asynchronous MAI. Finally, we point out that the proposed estimation and detection approach can be extended to impulse-modulation systems that deploy time hopping instead of DS-CDMA.

Appendix A
Interference Terms

In the multiuser asynchronous scenario, the MAI term at each DFT output reads

$$I_k(f_n) = \sum_{u=1}^{N_{\rm I}} \sum_{m=0}^{1} b_{k-m}^u G_{\rm EQ}^u(f_n, m), \qquad n = 0, \ldots, M-1, \quad f_n = \frac{n}{MT_{\rm c}}.$$

In fact, if we take as time reference the desired user's frame and we assume interferers with equal duration frames and code lengths, the DFT window partially overlaps two adjacent frames for each of the other users. The two frames of user u carry the information bits $b_{k-m}^u,\ m = 0, 1$. The bits are weighted after the DFT by

$$G_{\rm EQ}^u(f_n, 0) = T_{\rm c} \sum_{l=p_u}^{M-1} g_{\rm EQ}^u(lT_{\rm c} - p_u T_{\rm c} - \delta_u)\, {\rm e}^{-j2\pi f_n l T_{\rm c}},$$

$$G_{\rm EQ}^u(f_n, 1) = T_{\rm c} \sum_{l=0}^{p_u - 1} g_{\rm EQ}^u(lT_{\rm c} + MT_{\rm c} - p_u T_{\rm c} - \delta_u)\, {\rm e}^{-j2\pi f_n l T_{\rm c}}$$

where $\Delta_u = p_u T_{\rm c} + \delta_u$ is the time delay of user u that is assumed positive without loss of generality, and $|\delta_u| < T_{\rm c}$ is the fractional delay. $g_{\rm EQ}^u(t)$ is the equivalent-channel impulse response. Under the hypothesis of i.i.d. equally probable

information bits, and static users' time delay and channel, the MAI correlation matrix (in the absence of noise) has entries

$$\begin{aligned} R_{n,n'}(k,k) &= E\left[I_k(f_n)I_k^*(f_{n'})\right] \\ &= \sum_{u=1}^{N_\mathrm{I}} \sum_{m=0}^{1} G_{\mathrm{EQ}}^u(f_n,m) {G_{\mathrm{EQ}}^u}^*(f_{n'},m) \\ R_{n,n'}(k,k+1) &= R_{n',n}^*(k-1,k) \\ &= E\left[I_k(f_n)I_{k+1}^*(f_{n'})\right] \\ &= \sum_{u=1}^{N_\mathrm{I}} G_{\mathrm{EQ}}^u(f_n,0) {G_{\mathrm{EQ}}^u}^*(f_{n'},1) \end{aligned}$$

where the expectation is taken over the information bits. If all users are synchronous with the desired user, then the interference term becomes $I_k(f_n) = \sum_{u=1}^{N_\mathrm{I}} b_k^u G_{\mathrm{EQ}}^u(f_n,0)$ with $\Delta_u = \delta_u = p_u = 0$. In this case, $R_{n,n'}(k,l) = 0$, for $k \neq l$, while $R_{n,n'}(k,k)$ has entries $R_{n,n'}(k,k) = \sum_{u=1}^{N_\mathrm{I}} G_{\mathrm{EQ}}^u(f_n,0) {G_{\mathrm{EQ}}^u}^*(f_{n'},0)$.

Appendix B
Derivation of Metric (16)

Let us start from the (real) discrete-time received-signal model that is obtained from (11)

$$y(nT_\mathrm{c}) = \sum_k b_k g_{\mathrm{EQ}}(nT_\mathrm{c} - kT_\mathrm{f}) + z(nT_\mathrm{c})$$

where the interference plus noise is modeled with a zero-mean colored-Gaussian process $z(nT_\mathrm{c})$ (nonnecessarily stationary) with correlation function $r(nT_\mathrm{c}, lT_\mathrm{c}) = E[z(nT_\mathrm{c})z(lT_\mathrm{c})]$. With this model, under the knowledge of the channel, the maximum-likelihood receiver searches for the sequence of transmitted bits $\{\hat{b}_k\}$ (belonging to the desired user) that maximizes the logarithm of the probability density function of the received signal $\mathbf{y} = [\cdots y(0) y(T_\mathrm{c}) \cdots]$ conditional on a given hypothetical transmitted bit sequence, i.e., $\log p(\mathbf{y}|\{\hat{b}_k\})$. It follows that we have to search for the bit sequence of the desired user that maximizes the following log-likelihood function [19], [20]

$$\begin{aligned} \Lambda\left(\{\hat{b}_k\}\right) = -\sum_{l=-\infty}^{\infty} \sum_{m=-\infty}^{\infty} &\left(y(lT_\mathrm{c}) - \sum_k \hat{b}_k g_{\mathrm{EQ}}(lT_\mathrm{c} - kT_\mathrm{f})\right) \\ &\times \mathbf{K}_{l,m}^{-1} \left(y(mT_\mathrm{c}) - \sum_{k'} \hat{b}_{k'} g_{\mathrm{EQ}}(mT_\mathrm{c} - k'T_\mathrm{f})\right) \end{aligned}$$

where $\mathbf{K}_{l,m}^{-1}$ is the element of indices (l,m) of the inverse of the matrix $\mathbf{K} = E[\mathbf{z}\mathbf{z}^\mathrm{T}]$ with $\mathbf{z} = [\cdots\ z(0)\ z(T_\mathrm{c})\ \cdots]$. If we define the vector $\mathbf{e} = [\cdots\ e(0)\ e(T_\mathrm{c})\ \cdots]$, with $e(lT_\mathrm{c}) = y(lT_\mathrm{c}) - \sum_k \hat{b}_k g_{\mathrm{EQ}}(lT_\mathrm{c} - kT_\mathrm{f})$, the above function can be written as the following scalar product $\Lambda(\{\hat{b}_k\}) = -\mathbf{e}^\dagger \mathbf{K}^{-1}\mathbf{e} = -\langle \mathbf{e}, \mathbf{K}^{-1}\mathbf{e}\rangle$.

Since the scalar product is irrelevant to an orthonormal transform (Parseval theorem), we have that $\Lambda(\{\hat{b}_k\}) = -\langle \tilde{\mathbf{F}}\mathbf{e}, \tilde{\mathbf{F}}\mathbf{K}^{-1}\mathbf{e}\rangle$, with $\tilde{\mathbf{F}}$ being the block-diagonal orthonormal matrix that has blocks all identical to the M-point DFT matrix $\mathbf{F}$. Since, in our hypothesis, $g_{\mathrm{EQ}}(nT_\mathrm{c})$ has support in $[0, MT_\mathrm{c})$, the vector $\mathbf{E} = \tilde{\mathbf{F}}\mathbf{e}$ can be partitioned into nonoverlapping blocks equal to $\mathbf{E}_k = \mathbf{Y}_k - \hat{b}_k \mathbf{G}_{\mathrm{EQ}}$, i.e., the M-point DFT of the kth received frame minus the DFT of the hypothesized signal. It follows that

$$\begin{aligned} \Lambda(\{\hat{b}_k\}) &= -\langle \mathbf{E}, \tilde{\mathbf{F}}\mathbf{K}^{-1}\tilde{\mathbf{F}}^\dagger \mathbf{E}\rangle \\ &= -\langle \mathbf{E}, \mathbf{R}^{-1}\mathbf{E}\rangle \\ &= -\sum_{k=-\infty}^{\infty} \sum_{m=-\infty}^{\infty} [\mathbf{Y}_k - \hat{b}_k \mathbf{G}_{\mathrm{EQ}}]^\dagger \\ &\quad \times \mathbf{R}^{-1}(k,m)[\mathbf{Y}_m - \hat{b}_m \mathbf{G}_{\mathrm{EQ}}] \end{aligned}$$

where we have used the identity $\tilde{\mathbf{F}}\mathbf{K}\tilde{\mathbf{F}}^\dagger = E[\tilde{\mathbf{F}}\mathbf{z}\mathbf{z}^\mathrm{T}\tilde{\mathbf{F}}^\dagger] = E[\mathbf{Z}\mathbf{Z}^\dagger] = \mathbf{R}$, and $\mathbf{R}^{-1}(k,m)$ is the $M \times M$ block of indices (k,m) of $\mathbf{R}^{-1}$. The above result proves the metric in (16).

References

[1] M. Z. Win and R. A. Scholtz, "Impulse radio: How it works," *IEEE Commun. Lett.*, vol. 2, no. 1, pp. 10–12, Jan. 1998.

[2] G. Durisi and S. Benedetto, "Performance evaluation and comparison of different modulation schemes for UWB multiple access," in *Proc. IEEE Int. Conf. Communications (ICC)*, Anchorage, AK, May 2003, pp. 2187–2191.

[3] D. Porcino and W. Hirt, "Ultra-wideband radio technology: Potential and challenges ahead," *IEEE Commun. Mag.*, vol. 41, no. 7, pp. 66–74, Jul. 2003.

[4] J. R. Foerster, "The performance of direct-sequence spread ultra wideband system in the presence of multipath, narrowband interference, and multiuser interference," in *Proc. IEEE Conf. Ultra Wideband Systems and Technologies (UWBST)*, Baltimore, MD, May 2002, pp. 87–91.

[5] Q. Li and L. A. Rush, "Multiuser detection for DS-CDMA UWB in the home environment," *IEEE J. Sel. Areas Commun.*, vol. 20, no. 9, pp. 1701–1711, Dec. 2002.

[6] J. D. Choi and W. E. Stark, "Performance of ultra-wideband communications with suboptimal receivers in multipath channels," *IEEE J. Sel. Areas Commun.*, vol. 20, no. 9, pp. 1754–1766, Dec. 2002.

[7] M. Z. Win and R. A. Scholtz, "Characterization of ultra-wide bandwidth wireless indoor channels: A communication-theoretic view," *IEEE J. Sel. Areas Commun.*, vol. 20, no. 9, pp. 1613–1627, Dec. 2002.

[8] Y. Li, A. F. Molisch, and J. Zhang, "Channel estimation and signal detection for UWB," in *Proc. Wireless Personal Multimedia Communications Symp. (WPMC)*, Yokosuka, Japan, Oct. 2003, vol. 2, pp. 121–125.

[9] V. Lottici, A. D'andrea, and U. Mengali, "Channel estimation for ultra-wideband communications," *IEEE J. Sel. Areas Commun.*, vol. 20, no. 9, pp. 1638–1645, Dec. 2002.

[10] S. Verdu, *Multiuser Detection*. Cambridge, U.K.: Cambridge Univ. Press, 1998.

[11] S. Kaiser, "OFDM code-division multiplexing in fading channels," *IEEE Trans. Commun.*, vol. 50, no. 8, pp. 1266–1273, Aug. 2002.

[12] M. V. Clark, "Adaptive frequency-domain equalization and diversity combining for broadband wireless communications," *IEEE J. Sel. Areas Commun.*, vol. 16, no. 8, pp. 1385–1395, Oct. 1998.

[13] J. G. Proakis, *Digital Communications*, 3rd ed. New York: McGraw-Hill, 1995.

[14] K. J. Molnar and G. E. Bottomley, "Adaptive array processing MLSE receivers for TDMA digital cellular/PCS communications," *IEEE J. Sel. Areas Commun.*, vol. 16, no. 8, pp. 1340–1351, Oct. 1998.

[15] J. H. Winters, "Signal acquisition and tracking with adaptive arrays in digital mobile radio system IS-54 with flat fading," *IEEE Trans. Veh. Technol.*, vol. 42, no. 4, pp. 377–384, Nov. 1993.

[16] A. M. Tonello, "Iterative MAP detection of coded M-DPSK signals in fading channels with application to IS-136 TDMA," in *Proc. IEEE Vehicular Technology Conf. (VTC)—Fall*, Amsterdam, The Netherlands, Sep. 1999, pp. 1615–1619.

[17] ——, "Array processing for simplified turbo decoding of interleaved space–time codes," in *Proc. IEEE Vehicular Technology Conf. (VTC)—Fall*, Atlantic City, NJ, Oct. 2001, pp. 1304–1308.

[18] J. R. Foerster and Q. Li, "UWB channel modelling contribution from Intel, contribution to IEEE 802.15 Wireless Personal Area Networks," IEEE P802.15-02/279r0-SG3a, Intel Corp., Hillsboro, OR, Dec. 2003. [Online]. Available: http://ieee802.org/15

[19] M. Schwartz, "Abstract vector spaces applied to problems in detection and estimation theory," *IEEE Trans. Inf. Theory*, vol. IT-12, no. 3, pp. 327–336, Jul. 1966.

[20] G. Ungerboeck, "Adaptive maximum likelihood receiver for carrier-modulated data transmission systems," *IEEE Trans. Commun.*, vol. COMM-22, no. 5, pp. 624–636, May 1974.

[21] R. L. Cupo, G. D. Golden, C. C. Martin, K. L. Sherman, N. R. Sollemberger, J. H. Winters, and P. W. Wolniansky, "A four element adaptive antenna array for IS-136 PCS base stations," in *IEEE Proc. Vehicular Technology Conf. (VTC)*, Phoenix, AZ, May 1997, pp. 1577–1581.

Andrea M. Tonello (S'00–M'02) received the Doctor of Engineering degree in electronics (*cum laude*) in 1996, and the Doctor of Research degree in electronics and telecommunications in 2002, both from the University of Padova, Italy.

On February 1997, he joined as a Member of Technical Staff, Bell Labs—Lucent Technologies, where he worked on the development of baseband algorithms for cellular handsets first in Holmdel, NJ, and then within the Philips/Lucent Consumer Products Division in Piscataway, NJ. From September 1997 to December 2002, he has been with the Bell Labs Advanced Wireless Technology Laboratory, Whippany, NJ. He was promoted in 2002 to Technical Manager, and was appointed Managing Director of Bell Laboratories Italy. He has been on leave from his position for part of the period covered by September 1999–March 2002, while at the University of Padova, Italy. On January 2003, he joined the Dipartimento di Ingegneria Elettrica, Gestionale e Meccanica (DIEGM) of the University of Udine, Italy, where he is currently an Assistant Professor (*ricercatore*). He is the author of several papers and patents. He has been involved in the standardization activity for the evolution of the IS-136 Time-Division-Multiple-Access (TDMA) technology within Universal Wireless Communications Consortium (UWCC)/Telecommunications Industry Association (TIA). His research interests include wireless and powerline communications.

Dr. Tonello received a Lucent Bell Laboratories Recognition of Excellence Award for his work on enhanced receiver techniques. He is member of the IEEE Communications Society Broadband over Power Lines technical subcommittee.

Roberto Rinaldo (S'90–M'92) obtained the "Laurea in Ingegneria Elettronica" degree in 1987 from the University of Padova, Padova, Italy. From 1990 to 1992, he was with the University of California at Berkeley, where he received the M.S. degree in 1992. He received the Doctor of Research Degree in "Ingegneria Elettronica e dell'Informazione" from the University of Padova in 1992.

Since 1992, he has been with the Dipartimento di Elettronica e Informatica, University of Padova, first as an Assistant Professor (*ricercatore*), and then as an Associate Professor starting November 1, 1998. In November 2001, he joined the Faculty of the University of Udine, Udine, Italy, where he is currently a Professor in Communications and Signal Processing in the Dipartimento di Ingegneria Elettrica, Gestionale e Meccanica (DIEGM). His interests are in the field of multidimensional signal processing, video-signal coding, fractal theory, and image coding.